

## Positronium formation in positron-helium scattering

Pritikana Khan

*Muralidhar Girls' School, 4 Hindustan Road, Calcutta 700029, West Bengal, India*

A. S. Ghosh

*Department of Theoretical Physics, Indian Association for the Cultivation of Science,  
Jadavpur, Calcutta 700032, West Bengal, India*

(Received 29 October 1982)

The positronium-formation cross sections in positron-helium scattering have been calculated with the use of a distorted-wave polarized-orbital method from the threshold to 100 eV. The results with and without the matrix elements involving the distorted target wave functions are found to differ appreciably. The results of the first Born approximation are not expected to be correct even at the incident-positron energy 100 eV. The measured values at 20 eV are found to be less than  $\frac{1}{2}$  of the present predicted values. The sharp rise of the formation cross section within the ore-gap region as observed by Charlton *et al.* has also been noticed by us. The minimum in the differential cross section has been found at all energies as in the case of hydrogen atom.

### I. INTRODUCTION

In view of the recent estimates of the positronium (Ps)-formation cross section in the  $e^+$ -atom and  $e^+$ -molecule scattering by different groups,<sup>1,2</sup> much interest has been focused to investigate the problem theoretically. Moreover, the Ps-formation cross sections are important in some problem of astrophysics. Here we consider the formation of Ps-atom in  $e^+$ -He scattering from the threshold to 100 eV.

Theoretically few attempts have been made to calculate the Ps formation in  $e^+$ -atom scattering. In the case of the hydrogen atom there are some reliable calculations<sup>3</sup> of the formation cross section in the ore-gap region. This has helped to find a tractable method to investigate the problem. In the case of helium, no such calculations have been performed. Apart from some first-order calculations suitable at high incident energies, the coupled state calculations were performed by Mandal *et al.*<sup>4</sup> for few partial waves. Mandal *et al.*<sup>5</sup> have repeated their coupled-state calculation in which the effects of target distortion are included in both the channel and in the framework of adiabatic approximation. A distorted-wave method in which the incident wave is obtained in the static approximation was applied by Mandal *et al.*<sup>6</sup> to investigate the same problem. However, at the incident-positron energy of 40

eV, the incident wave used by them is an adiabatic one. The first Born results at 20 eV is approximately 20 times higher than that of the experimental estimate. The distorted-wave results of Mandal *et al.*<sup>6</sup> are very close to the measured values of the Wayne State University group<sup>2</sup> as well as of the University College London group.<sup>1</sup> This is rather surprising due to the fact that the method of Mandal *et al.*<sup>6</sup> does not take the effects of target distortion and of Ps formation in the incident channel. Moreover, the steep rise of their Ps-formation cross section beyond the ore-gap region contradicts the primary findings of Charlton *et al.*<sup>7</sup>

Here we have extended our earlier polarized orbital calculations<sup>8</sup> for the Ps-formation cross section in  $e^+$ -H scattering to investigate the  $e^+$ -He scattering. The Ps-formation cross sections in  $e^+$ -H scattering as obtained by us<sup>8</sup> are in good agreement with those of elaborate methods.<sup>2</sup> Our incident wave contains the effect of the dipole polarization potential having the exact polarizability. The deficiency due to the noninclusion of the Ps-formation channel is partially compensated due to the inclusion of the exact dipole polarizability. We have also included in our calculation the matrix elements containing the distorted target wave functions. It has been found<sup>8</sup> that these matrix elements are important in the calculation of cross sections.

## II. THEORY

Let  $\vec{r}_1, \vec{r}_2, \vec{r}_3$  be the position vectors of the incident positron and the bound electrons with respect to the nucleus. The polarized-orbital wave function for the system of the incident positron and helium atom is given by

$$\begin{aligned}\Psi_i(\vec{r}_1, \vec{r}_2, \vec{r}_3) &= \{ [u(\vec{r}_2) + \Phi_d(\vec{r}_1, \vec{r}_2)] [u(\vec{r}_3) + \Phi_d(\vec{r}_1, \vec{r}_3)] \} F(\vec{r}_1) \\ &= [u(\vec{r}_2)u(\vec{r}_3) + u(\vec{r}_2)\Phi_d(\vec{r}_1, \vec{r}_3) + u(\vec{r}_3)\Phi_d(\vec{r}_1, \vec{r}_2) + \Phi_d(\vec{r}_1, \vec{r}_2)\Phi_d(\vec{r}_1, \vec{r}_3)] F(\vec{r}_1).\end{aligned}$$

As we are retaining first-order term, the second-order term

$$\Phi_d(\vec{r}_1, \vec{r}_2)\Phi_d(\vec{r}_1, \vec{r}_3)$$

may be neglected. Therefore  $\Psi_i(\vec{r}_1, \vec{r}_2, \vec{r}_3)$  takes the form

$$\begin{aligned}\Psi_i(\vec{r}_1, \vec{r}_2, \vec{r}_3) &= [\Phi_{\text{He}}(\vec{r}_2, \vec{r}_3) + u(\vec{r}_2)\Phi_d(\vec{r}_1, \vec{r}_3) \\ &\quad + u(\vec{r}_3)\Phi_d(\vec{r}_1, \vec{r}_2)] F(\vec{r}_1),\end{aligned}\quad (1)$$

where  $\Phi_{\text{He}}(\vec{r}_2, \vec{r}_3) = u(\vec{r}_2)u(\vec{r}_3)$  with  $u(r)$  is given by<sup>9</sup>

$$u(r) = \frac{N}{\sqrt{\pi}} (e^{-z_1 r} + C e^{-2z_1 r}).\quad (2)$$

In the framework of the one-electron approximation,  $\Phi_d(\vec{x}, \vec{r})$  takes the form

$$\Phi_d(\vec{x}, \vec{r}) = -\frac{1}{\sqrt{\pi}} \frac{\epsilon(x, r)}{x^2} \frac{u_{1s \rightarrow p}(r)}{r} P_1(\cos\theta_{xr}),\quad (3)$$

where

$$\epsilon(x, r) = \begin{cases} 1, & x > r \\ 0, & x < r \end{cases}$$

and

$$U_{1s \rightarrow p}(r) = (Z_p)^{1/2} e^{-Z_p r} (\frac{1}{2} Z_p r^3 + r^2)$$

with  $Z_p = 1.594$ . The value of  $Z_p$  is so chosen that it gives the exact polarizability.

The scattering amplitude for the positronium formation in its ground state is given by

$$\begin{aligned}f(\theta) &= -\frac{1}{2} \left[ \frac{\mu_f}{2\pi} \right] \\ &\quad \times \langle \Phi_{\text{Ps}}^*(\vec{r}_1, \vec{r}_2) \Phi_{\text{He}^+}^*(\vec{r}_3) | V_f | \Psi_i(\vec{r}_1, \vec{r}_2, \vec{r}_3) \rangle,\end{aligned}\quad (4)$$

where

$$\begin{aligned}\Phi_{\text{Ps}}^*(\vec{r}_1, \vec{r}_2) &= \eta^*(|\vec{r}_1 - \vec{r}_2|) \\ &\quad \times \exp[-\frac{1}{2} i \vec{k}_{\text{Ps}} \cdot (\vec{r}_1 + \vec{r}_2)]\end{aligned}\quad (5)$$

and  $\mu_f$  is the reduced mass in the final channel.

Here  $\eta^*(|\vec{r}_1 - \vec{r}_2|)$  is the ground-state wave function of the positronium atom and  $V_f$  is the interaction potential in the final channel and takes the form

$$V_f = \left[ \frac{Z_A}{r_1} - \frac{Z_A}{r_2} - \frac{1}{r_{12}} + \frac{1}{r_{23}} \right].$$

The positron scattering wave function  $F(r_1)$  may be written as

$$F(r_1) = \frac{1}{\sqrt{K_i}} \sum_{l=0}^{\infty} (2l+1) i^l e^{i\delta_l} \frac{u_l(r_1)}{r_1} P_L(\cos\theta_{r_1})\quad (6)$$

and  $u_l$  satisfies the differential equation

$$\left[ \frac{d^2}{dr_1^2} + k_i^2 - V_s(r_1) - V_d(r_1) - \frac{l(l+1)}{r_1^2} \right] u_l(r_1) = 0,\quad (7)$$

where  $V_s$  is the static potential and  $V_d$  is the polarization potential.

The scattering amplitude given by the expression (4) may be written as

$$f(\theta) = f_1(\theta) + f_2(\theta) + f_3(\theta),$$

where

$$\begin{aligned}f_1(\theta) &= -\frac{1}{2} \left[ \frac{\mu_f}{2\pi} \right] \int \omega^*(\vec{R}) \eta^*(s) \Phi_{\text{He}^+}^*(\vec{r}_3) V_f \\ &\quad \times \Phi_{\text{He}}(\vec{r}_2, \vec{r}_3) \\ &\quad \times F(\vec{r}_1) d\vec{r}_1 d\vec{r}_2 d\vec{r}_3,\end{aligned}\quad (8)$$

$$\begin{aligned}f_2(\theta) &= -\frac{1}{2} \left[ \frac{\mu_f}{2\pi} \right] \int \omega^*(\vec{R}) \eta^*(s) \Phi_{\text{He}^+}^*(\vec{r}_3) V_f u(\vec{r}_3) \\ &\quad \times \Phi_d(\vec{r}_1, \vec{r}_2) F(\vec{r}_1) d\vec{r}_1 d\vec{r}_2 d\vec{r}_3,\end{aligned}\quad (9)$$

and

TABLE I. *s*-wave positronium-formation cross section in units of  $\pi a_0^2$ .

Energy (eV)	Present results			Mandal <i>et al.</i> <sup>a</sup>	
	Born	Adiabatic	Polarized orbital	Static	Adiabatic
19.0	1.123 16	0.125 59	0.156 58		
20.0	1.324 80	0.135 68	0.172 08	0.006 19	
24.5	1.333 03	0.096 06	0.130 62	0.003 64	
28.0	1.134 21	0.064 05	0.091 29	0.002 36	
40.0	0.608 30	0.018 85	0.029 84	0.000 12	0.037 70
60.0	0.239 62	0.002 54	0.001 77	0.000 15	
100.0	0.047 67	0.000 47	0.000 40	0.002 08	

<sup>a</sup> Reference 6.

$$f_3(\theta) = -\frac{1}{2} \left[ \frac{\mu_f}{2\pi} \right] \int \omega^*(\vec{R}) \eta^*(s) \Phi_{\text{He}^+}^*(\vec{r}_3) V_f u(\vec{r}_2) \times \Phi_d(\vec{r}_1, \vec{r}_3) F(\vec{r}_1) d\vec{r}_1 d\vec{r}_2 d\vec{r}_3. \quad (10)$$

The final expressions for  $f_i(\theta)$  are given in Appendix A. The first Born scattering amplitude is obtained by replacing  $F(r_1)$  by a plane wave in  $f_1(\theta)$ . The first Born approximation (FBA) amplitudes may also be obtained without breaking into partial waves. The expression for the FBA amplitude is given in Appendix B.

The para-Ps-formation cross section  $\sigma_{\text{Ps}}^{\text{para}}$  is expressed as

$$\sigma_{\text{Ps}}^{\text{para}} = 2\pi \left[ \frac{k_f}{k_i} \right] \int_0^\pi |f(\theta)|^2 \sin\theta d\theta. \quad (11)$$

The total Ps-formation cross section is given by

$$\sigma_{\text{Ps}} = 4\sigma_{\text{Ps}}^{\text{para}}. \quad (12)$$

In the case of the FBA we replace  $f(\theta)$  by  $f^{\text{FBA}}(\theta)$  in the relation (11).

### III. RESULTS AND DISCUSSION

The FBA amplitude may be obtained from the expression (A1) by replacing  $u_i(r)/r$  by  $j_l(k_i r)$ . The results of the FBA have been calculated by using the expression (B1) as well as the expression (A1). Two results are found to be identical at 20.0 and 24.5 eV. This serves as a check of our numerical accuracy. We have calculated the matrix element containing the distorted target wave function for the partial waves  $l \leq 2$ , and for  $l=3$  and 4 the matrix element  $f_1(\theta)$  (adiabatic) has only been calculated. The contributions from higher partial waves have been replaced by

$$f^{\text{FBA}} = \sum_{l=0}^4 f_l^{\text{FBA}}.$$

Here  $f_l^{\text{FBA}}$  denotes the partial-wave form of Born amplitude.

Our *s*-, *p*-, *d*-, *f*-, and *g*-wave cross sections are given in Tables I–V. The adiabatic results of Mandal *et al.*<sup>6</sup> at 40 eV differ from the present results appreciably. The difference is attributed to the fact that Mandal *et al.*<sup>6</sup> used the value of induced dipole polarizability to be 1.10 a.u. whereas our value is ex-

TABLE II. *p*-wave positronium-formation cross section in units of  $\pi a_0^2$ .

Energy (eV)	Present results			Mandal <i>et al.</i> <sup>a</sup>	
	Born	Adiabatic	Polarized orbital	Static	Adiabatic
19.0	0.016 05	0.012 06	0.008 81		
20.0	0.031 19	0.024 64	0.017 40	0.058 34	
24.5	0.060 556	0.055 54	0.036 69	0.132 20	
28.0	0.055 98	0.058 45	0.036 41	0.141 00	
40.0	0.029 07	0.047 62	0.025 83	0.098 86	0.052 15
60.0	0.010 35	0.028 80	0.141 11	0.046 12	
100.0	0.000 78	0.006 33	0.001 92	0.014 47	

<sup>a</sup> Reference 6.

TABLE III. *d*-wave positronium-formation cross section in units of  $\pi a_0^2$ .

Energy (eV)	Present results			Mandal <i>et al.</i> <sup>a</sup>	
	Born	Adiabatic	Polarized orbital	Static	Adiabatic
19.0	0.006 36	0.005 55			
20.0	0.022 17	0.019 28	0.016 28	0.023 73	
24.5	0.120 75	0.104 05	0.099 02	0.129 70	
28.0	0.165 86	0.142 25	0.135 37	0.180 70	
40.0	0.134 15	0.114 74	0.108 72	0.177 60	0.147 70
60.0	0.036 80	0.032 79	0.030 14	0.089 27	
100.0	0.001 94	0.002 86	0.002 15	0.024 48	

<sup>a</sup>Reference 6.

act. Therefore the Ps-formation cross sections are very sensitive to the choice of the long-range potential. The present two sets of the *s*-wave cross sections are large in the ore-gap region compared to other partial-wave contributions. This feature has not been noticed in the case of the H atom. It is well known that the polarized-orbital wave function is not accurate for small values of *r*. Therefore the change in the *s*-wave values with the use of a more accurate wave function is expected. But this change in the *s*-wave values, we believe, will not be very appreciable. The results of the H atom<sup>7</sup> suggests that this feature may be attached to the particular property of the target system.

The results of the Born approximation is not valid for the lower partial waves as is evident from the tables. The Born partial-wave contribution may be used beyond the partial waves given in the table. The similar features has also been found by us<sup>8</sup> for the case of the hydrogen atom. Moreover, the Ps-formation cross section at 100 eV is about 50% higher than the present polarized-orbital results (Table VI). The contention that the first Born approximation is not valid for a rearrangement process at intermediate energies is also clear in this calculation.

The differential cross sections at the three incident positron energies are given in Figs. 1–3. At

the incident energy 20 eV (Fig. 1) there is no minimum value of the Born differential cross section. This feature has also been noticed at 19 eV (not given in the figure). In the case of the hydrogen atom it has not been found at any incident energies. At 24.5 eV (Fig. 2) and 28.0 eV (Fig. 3) the minimum in the differential cross section has also been noticed using the Born approximation. The position of the minimum changes with the variation of energies and of the approximations used.

In Table VI we have tabulated the present two sets of total positronium-formation cross sections in the energy range 19.0 to 100.0 eV along with those of first Born and static results of Mandal *et al.*<sup>6</sup> By adiabatic results we mean the contribution of matrix element involving the ground-state wave function of the helium atom only. At 20.0 eV, the experimental estimate for the positronium-formation cross sections that have been extracted by subtracting the extrapolated (from below) values of the elastic cross sections from the total cross section are also given in the same table.

It is evident from the results that the present Ps-formation cross section rises very steeply up to the excitation threshold energy and the rate of rise is slowed down after this energy. On the other hand, steep rise of Ps-formation cross sections is predicted in the static approximation beyond the excitation

TABLE IV. *f*-wave positronium-formation cross section in units of  $\pi a_0^2$ .

Energy (eV)	Present results		Mandal <i>et al.</i> <sup>a</sup>	
	Born	Adiabatic	Static	Adiabatic
24.5	0.047 82	0.044 85	0.049 37	
28.0	0.090 95	0.084 86	0.092 58	
40.0	0.158 30	0.145 76	0.141 00	0.130 50
60.0	0.142 81	0.132 58	0.088 86	
100.0	0.078 48	0.075 89	0.026 45	

<sup>a</sup>Reference 6.TABLE V. *g*-wave positronium-formation cross section in units of  $\pi a_0^2$ .

Energy (eV)	Present results		Mandal <i>et al.</i> <sup>a</sup>	
	Born	Adiabatic	Static	Adiabatic
24.5	0.012 45	0.012 09	0.012 71	
28.0	0.030 40	0.029 42	0.032 30	
40.0	0.063 58	0.060 54	0.078 01	0.075 14
60.0	0.029 41	0.027 07	0.064 02	
100.0	0.000 35	0.000 22	0.022 26	

<sup>a</sup>Reference 6.

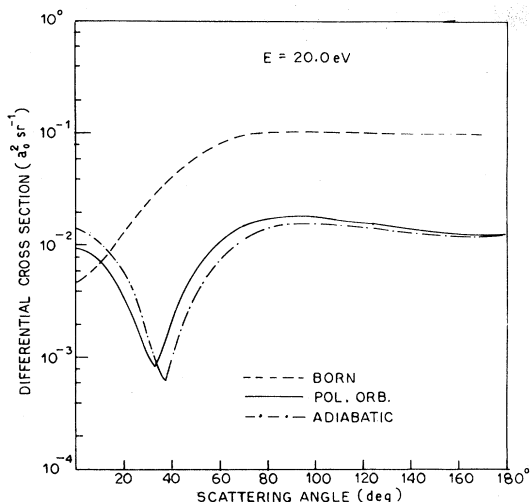


FIG. 1. Differential cross section for positronium formation in  $e^+$ -He scattering.

threshold. Charlton *et al.*<sup>7</sup> have observed that the Ps-formation cross section has reached its maximum value near the excitation threshold and decreases very slowly beyond this energy. As a consequence, the position of the maximum value of the formation cross section obtained theoretically is at a higher energy than that found experimentally.

The experimental estimates of the Ps-formation

cross section at the incident positron energy 20.0 eV differ appreciably from the present two sets of results. The static result of Mandal *et al.*<sup>6</sup> at this energy is surprisingly in good agreement with the measured value whereas the Born result is about 20 times the estimated value. The assumption that has been made in estimating the measured Ps-formation cross section may not be valid. The elastic cross section is expected to be influenced appreciable due to the opening of the Ps-formation channel and extrapolation of the elastic results may be questioned. However, the extrapolation of the elastic cross section through the threshold is supported at least for  $s$ -wave positron-hydrogen scattering by the three most accurate calculations of positronium formation. It may be added that the  $s$ -wave contribution to the positronium-formation cross section in  $e^+$ -H scattering is rather negligible compared to the total positronium cross section. Moreover, the agreement between the values of Mandal *et al.*<sup>6</sup> and experiment is rather purely accidental. In the case of the hydrogen atom, our results are in fair agreement with those of the most elaborate calculations. In absence of elaborate theoretical calculations and of direct measurements for the  $e^+$ -He system, it is not possible to judge the accuracy and validity of the present method. However, it is not expected that the present theory fails so miserably. The present calculations warrant elaborate theoretical calculations and direct measurement of positronium formation.

#### APPENDIX A: FINAL EXPRESSIONS FOR THE SCATTERING AMPLITUDES

The scattering amplitude  $f_1(\theta)$  is given by

$$f_1(\theta) = -\frac{1}{2} \left[ \frac{\mu_f}{2\pi} \right] \int \omega^*(\vec{R}) \eta^*(s) \Phi_{\text{He}^+}^*(\vec{r}_3) |V_f| \Phi_{\text{He}}(\vec{r}_2, \vec{r}_3) F(\vec{r}_1) d\vec{r}_1 d\vec{r}_2 d\vec{r}_3.$$

Using the partial-wave expression for  $\omega^*(\vec{R})$ ,  $\eta^*(s)$ ,  $V_f$ , and  $F(\vec{r}_1)$  and performing all the integrations except the radial integration over  $dr_1$ ,  $f_1(\theta)$  reduces to

TABLE VI. Total positronium-formation cross section in units of  $\pi a_0^2$ .

Energy (eV)	Present results				Griffith <sup>b</sup>	Stein <i>et al.</i> <sup>c</sup>
	Born	Adiabatic	Polarized orbital	Static <sup>a</sup>		
19.0	1.146 20	0.144 10	0.171 60			
20.0	1.381 89	0.183 30	0.209 40	0.092 10	0.07±0.03	0.08
24.5	1.576 81	0.314 88	0.325 46	0.330 30		
28.0	1.490 62	0.392 23	0.390 56	0.458 10		
40.0	1.038 32	0.432 40	0.415 60	0.544 90		
60.0	0.514 72	0.279 50	0.264 40	0.347 40		
100.0	0.144 15	0.100 69	0.095 50	0.129 00		

<sup>a</sup> Reference 6.

<sup>b</sup> Reference 1.

<sup>c</sup> Reference 2.

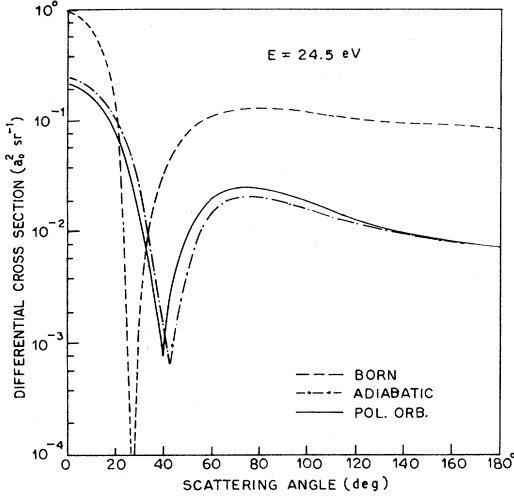


FIG. 2. Same as Fig. 1.

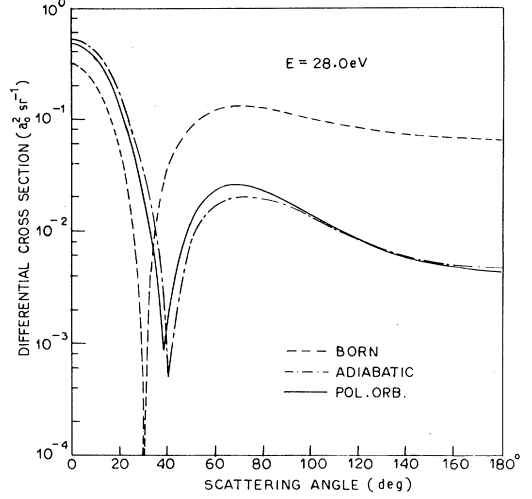


FIG. 3. Same as Fig. 1.

$$f_1(\theta) = -4\sqrt{2}N^2\pi \sum_{i=1}^2 a_i \sum_{j=1}^2 b_j \left[ \frac{2}{\lambda_i} (T_1 - T_2 + T_5 - T_6) + T_3 - T_4 \right] \frac{1}{\lambda_i^2} \quad (\text{A1})$$

with

$$T_1 = \alpha_j \sum_l (2l+1)^{1/2} e^{i\delta_l} y_{l0}(\hat{k}_f) \int dx x (1-x) \int e^{-u_1 r_1} F_1(r_1, u_1) \frac{u_l(r_1)}{r_1} j_l\left(\frac{1}{2}(2-x)k_f r_1\right) r_1 dr_1,$$

$$T_2 = \sum_l (2l+1)^{1/2} e^{i\delta_l} y_{l0}(\hat{k}_f) \int dx x \int e^{-\mu_1 r_1} Z_1(r_1, \mu_1) \frac{u_l(r_1)}{r_1} j_l\left(\frac{1}{2}(2-x)k_f r_1\right) r_1^2 dr_1,$$

$$T_3 = \alpha_j \sum_l (2l+1)^{1/2} e^{i\delta_l} y_{l0}(\hat{k}_f) \int dx x (1-x) \int e^{-(\mu_1 + \lambda_i) r_1} F_1(r_1, \mu_1) \frac{u_l(r_1)}{r_1} \\ \times j_l\left(\frac{1}{2}(2-x)k_f r_1\right) r_1^2 dr_1,$$

$$T_4 = (\alpha_j + \lambda_i) \sum_l (2l+1)^{1/2} e^{i\delta_l} y_{l0}(\hat{k}_f) \int dx x (1-x) \int e^{-\mu_2 r_1} F_2(r_1, \mu_2) \frac{u_l(r_1)}{r_1} \\ \times j_l\left(\frac{1}{2}(2-x)k_f r_1\right) r_1^2 dr_1,$$

$$T_5 = \alpha_j \sum_l (2l+1)^{1/2} e^{i\delta_l} y_{l0}(\hat{k}_f) \int dx x (1-x) \int e^{-(\mu_1 + \lambda_i) r_1} F_1(r_1, \mu_1) \frac{u_l(r_1)}{r_1} \\ \times j_l\left(\frac{1}{2}(2-x)k_f r_1\right) r_1 dr_1,$$

$$T_6 = \sum_l (2l+1)^{1/2} e^{i\delta_l} y_{l0}(\hat{k}_f) \int dx x \int e^{-\mu_2 r_1} Z_2(r_1, \mu_2) \frac{u_l(r_1)}{r_1} j_l\left(\frac{1}{2}(2-x)k_f r_1\right) r_1^2 dr_1,$$

where

$$F_1(r_1, \mu_1) = \frac{1}{\mu_1^3} \left[ \frac{3}{\mu_1^2} + \frac{3r_1}{\mu_1} + r_1^2 \right], \quad Z_1(r_1, \mu_1) = \frac{1}{\mu_1^2} \left[ \frac{1}{\mu_1} + r_1 \right], \quad \mu_1^2 = \frac{1}{4}x + \alpha_j^2(1-x) + \frac{1}{4}x(1-x)k_f^2,$$

and

$$F_2(r_1, \mu_2) = \frac{1}{\mu_2^3} \left[ \frac{3}{\mu_2^2} + \frac{3r_1}{\mu_2} + r_1^2 \right], \quad Z_2(r_1, \mu_2) = \frac{1}{\mu_2^2} \left[ \frac{1}{\mu_2} + r_1 \right],$$

$$\mu_2^2 = \frac{1}{4}x + (\alpha_j + \lambda_i)^2(1-x) + \frac{1}{4}x(1-x)k_f^2,$$

$$a_1 = 1, \quad b_1 = 1, \quad \alpha_1 = Z_i, \quad \lambda_1 = 2 + Z_i, \quad a_2 = 0.6, \quad b_2 = 0.6, \quad \alpha_2 = 2Z_1, \quad \lambda_2 = 2 + 2Z_1.$$

Similarly the final expressions for  $f_2(\theta)$  and  $f_3(\theta)$  are given by

$$\begin{aligned} f_2(\theta) = & 4\sqrt{2}N\sqrt{\pi} \sum_{l_1, l_2, l} (i)^{l-(l_1+l_2)} e^{i\delta_l} \frac{(2l_1+1)}{(2l+1)^{1/2}} Y_{l0}(\hat{k}_f) \\ & \times \left[ (2l_2+1) C \begin{matrix} l_1 & l_2 & l \\ 0 & 0 & 0 \end{matrix} \right]^2 \int j_{l_1}(\frac{1}{2}k_f r_1) j_{l_2}(\frac{1}{2}k_f r_3) G_{l_2}(r_1 \geq r_3) f'_1(r_1) \\ & \times (e^{-Z_i r_3} + 0.6e^{-2Z_i r_3}) \frac{u_l(r_1)}{r_1} r_1^2 r_3^2 dr_1 dr_3 \\ & - \sum_{\lambda} (2\lambda+1) C \begin{matrix} l_2 & l_1 & l \\ 0 & 0 & 0 \end{matrix} \right]^2 C \begin{matrix} \lambda & 1 & l_2 \\ 0 & 0 & 0 \end{matrix} \\ & \times \int dr_1 dr_3 r_3^2 (e^{-Z_i r_3} + 0.6e^{-2Z_i r_3}) g(r_1, r_3) G_{\lambda}(r_1 \geq r_3) \\ & \times j_{l_1}(\frac{1}{2}k_f r_1) j_{l_2}(\frac{1}{2}k_f r_3) \frac{u_l(r_1)}{r_1} \Big], \end{aligned} \quad (A2)$$

where

$$\begin{aligned} f'_1(r_1) = & \frac{8}{3} \left[ \frac{Z_A}{Z_p} \right]^{1/2} \frac{1}{r_1^4} \left[ \left[ -\frac{1}{2}Z_p \left[ \frac{e^{-\alpha r_1}}{\alpha} \left[ r_1^5 + \frac{5r_1^4}{\alpha} + \frac{20r_1^3}{\alpha^2} + \frac{60r_1^2}{\alpha^3} + \frac{120r_1}{\alpha^4} + \frac{120}{\alpha^5} \right] - \frac{120}{\alpha^6} \right] \right] \right. \\ & \left. + \left[ -\frac{e^{-\alpha r_1}}{\alpha} \left[ r_1^4 + \frac{4r_1^3}{\alpha} + \frac{12r_1^2}{\alpha^2} + \frac{24r_1}{\alpha^3} + \frac{24}{\alpha^4} \right] + \frac{24}{\alpha^5} \right] \right] \end{aligned}$$

with  $\alpha = Z_A + Z_p$ ,

$$G_{\lambda} = \left[ \frac{r_1}{r_3} \right]^{1/2} K'_{\lambda+1/2}(\frac{1}{2}r_1) I_{\lambda+1/2}(\frac{1}{2}r_3) + \left[ \frac{r_3}{r_1} \right]^{1/2} K_{\lambda+1/2}(\frac{1}{2}r_1) I_{\lambda+1/2}(\frac{1}{2}r_3)$$

and  $C \begin{matrix} \alpha & \beta & \gamma \\ \mu & \nu & \end{matrix}$  is the Clebsch-Gordan coefficient,<sup>10</sup> and

$$\begin{aligned} f_3(\theta) = & -128N\sqrt{\pi} \sum_{l_1, l_2, l, \lambda} (i)^{l-(l_1+l_2)} e^{i\delta_l} \left[ \frac{(2\lambda+1)(2l_1+1)}{(2l+1)^{1/2}} \right] Y_{J0}(\hat{k}_f) C \begin{matrix} l_2 & l_1 & l \\ 0 & 0 & 0 \end{matrix} \right]^2 C \begin{matrix} \lambda & l_1 & l_2 \\ 0 & 0 & 0 \end{matrix} \\ & \times \int dr_1 dr_3 r_3^2 Z(r_1, r_3) u_{1s \rightarrow p}(r_3) G_{\lambda}(r_1 \geq r_3) j_{l_1}(\frac{1}{2}k_f r_1) j_{l_2}(\frac{1}{2}k_f r_3) \frac{u_l(r_1)}{r_1}, \end{aligned} \quad (A3)$$

where

$$Z(r_1, r_3) = W(r_1) - P(r_3)$$

with

$$W(r_1) = 16\sqrt{2\pi} \frac{N}{\sqrt{\pi}} \left[ \frac{1}{r_1} \left[ \frac{1}{\alpha_1^3} + \frac{c}{\alpha_2^3} \right] + \frac{1}{\alpha_1^3} \left[ \frac{1}{r_1} + \frac{\alpha_1}{2} \right] e^{-\alpha_1 r_1} + \frac{c}{\alpha_2^3} \left[ \frac{1}{r_1} + \frac{\alpha_2}{2} \right] e^{-\alpha_2 r_1} \right]$$

and

$$P(r_3) = 16\sqrt{2\pi} \frac{N}{\sqrt{\pi}} \left[ \frac{1}{r_3} \left[ \frac{1}{\alpha_1^3} + \frac{c}{\alpha_2^3} \right] + \frac{1}{\alpha_1^3} \left[ \frac{1}{r_3} + \frac{\alpha_1}{2} \right] e^{-\alpha_1 r_3} + \frac{c}{\alpha_2^3} \left[ \frac{1}{r_3} + \frac{\alpha_2}{2} \right] e^{-\alpha_2 r_3} \right].$$

### APPENDIX B: EVALUATION OF THE FBA SCATTERING AMPLITUDE

The FBA scattering amplitude is given by

$$f^{\text{FBA}}(\theta) = -\frac{1}{2\pi} \int \Phi_{\text{He}^+}^*(\vec{r}_2) \omega^*(r_{12}) \exp \left[ -i \vec{k}_f \cdot \left( \frac{\vec{r}_1 + \vec{r}_2}{2} \right) \right] V_{\text{int}} \Phi_{\text{He}}(\vec{r}_2, \vec{r}_3) e^{i \vec{k}_i \cdot \vec{r}_1} d\vec{r}_1 d\vec{r}_2 d\vec{r}_3.$$

After performing the integration over  $d\vec{r}_1$ ,  $d\vec{r}_2$ , and  $d\vec{r}_3$ , the scattering amplitude  $f^{\text{FBA}}(\theta)$  reduces to

$$f^{\text{FBA}}(\theta) = -\frac{2N^2}{\pi^2} \sum_{i=1}^2 a_i \sum_{j=1}^2 b_j \left[ \frac{2}{\lambda_i^3} (I_5 - I_6) + \frac{1}{\lambda_i^2} (I_3 - I_4) + \frac{2}{\lambda_i^3} (I_1 - I_2) \right], \quad (\text{B1})$$

where

$$I_6 = 32\pi^2 \int_0^1 \frac{x dx}{(\omega^2 + \mu^2)^3}$$

with

$$|\omega| = \left| \vec{k}_i - \frac{2-x}{2} \vec{k}_f \right|,$$

$$\mu^2 = \frac{1}{4}x + (\alpha_j + \lambda_i)^2(1-x) + \frac{1}{4}x(1-x)k_f^2,$$

$$I_5 = 4\pi^2 \alpha_j \int_0^1 dx x(1-x) \left[ \frac{3A_1^2 + 2\mu(3\mu_1 - \mu)A_1 + 8\mu_1^2\mu^2}{\mu^5 A_1^3} \right]$$

with

$$A_1 = \omega^2 + \mu_1^2, \quad \mu_1 = \mu + \lambda_i,$$

and

$$\mu^2 = \frac{1}{4}x + \alpha_j^2(1-x) + \frac{1}{4}x(1-x)k_f^2,$$

$$I_4 = 192\pi^2 \int_0^1 dx x(1-x) \left[ \frac{(\alpha_j + \lambda_i)}{\omega^2 + \mu^2} \right],$$

$$I_3 = 4\pi^2 \alpha_j \int_0^1 dx x(1-x) \left[ \frac{6\lambda_1 A_1^2 + 24\mu\mu_1(\lambda_i A_1 + 2\mu\mu_1^2)}{\mu^5 A_1^4} \right],$$

$$I_2 = 32\pi^2 \int_0^1 \frac{x dx}{(\omega^2 + \mu^2)^3}$$



with

$$\mu^2 = \frac{1}{4}x + \alpha_j^2(1-x) + \frac{1}{4}x(1-x)k_f^2,$$

$$I_1 = 4\pi^2\alpha_j \int_0^1 dx x(1-x) \left[ \frac{3(\omega^2 + \mu^2) + 4\mu^2(\omega^2 + \mu^2) + 8\mu^4}{\mu^5(\omega^2 + \mu^2)^3} \right].$$

The values of  $a_i$ ,  $b_i$ ,  $\alpha_i$ , and  $\lambda_i$  are given in Appendix A.

<sup>1</sup>T. C. Griffith and G. R. Heyland, *Phys. Rep.* **39C**, 69 (1978).

<sup>2</sup>T. S. Stein, W. E. Kauppila, V. Pol, J. H. Smart, and G. Jesion, *Phys. Rev. A* **17**, 1600 (1978).

<sup>3</sup>Y. F. Chan and P. A. Fraser, *J. Phys. B* **6**, 2504 (1973); J. Stein and R. Sternlich, *Phys. Rev. A* **6**, 2165 (1972); J. W. Humberston, *Can. J. Phys.* **60**, 591 (1982).

<sup>4</sup>P. Mandal, A. S. Ghosh, and N. C. Sil, *J. Phys. B* **8**, 14 (1975).

<sup>5</sup>P. Mandal, D. Basu, and A. S. Ghosh, *J. Phys. B* **9**, 2633

(1976).

<sup>6</sup>P. Mandal, S. Guha, and N. C. Sil, *J. Phys. B* **12**, 17 (1979).

<sup>7</sup>M. Charlton, T. C. Griffith, G. R. Heyland, K. S. Lines, and G. L. Wright, *J. Phys. B* **13**, L757 (1980).

<sup>8</sup>P. Khan and A. S. Ghosh, *Phys. Rev. A* **27**, 1904 (1983).

<sup>9</sup>L. G. Green, M. M. Mulder, M. N. Lewis, and J. W. Wall, *Phys. Rev.* **93**, 757 (1954).

<sup>10</sup>M. E. Rose, *Elementary Theory of Angular Momentum* (Wiley, New York, 1963).